Hierarchical Coordination of Two-Time Scale Microgrids With Supply-Demand Imbalance

Yigao Du, Jing Wu, *Member, IEEE*, Shaoyuan Li, *Senior Member, IEEE*, Chengnian Long, *Member, IEEE*, and Simona Onori, *Senior Member, IEEE*

***Abstract*—This paper focuses on the energy management problem for Autonomous MicroGrids (AMGs), where internal demand may exceed internal power supply provided by Renewable Energy Sources (RESs) and Battery Energy Storage Systems (BESSs). To derive a balance for the mismatched demand response and energy supply, a three level hierarchical coordination strategy is proposed. The top level is responsible for energy coordination between the Distribution Network Operator (DNO) and AMGs. The DNO will purchase/sell energy from/to an AMG that has surplus/deficient energy at a slow sampling period. The medium level focuses on the local balance of each individual AMG, which optimizes the charge/discharge energy of BESSs and dispatches of the aggregator with the same sampling period as the top level. The bottom level will make load cutting decisions according to the optimization results of the medium level in the case of supply-demand imbalance, which is updated of a fast sampling rate. Furthermore, the two-time scale optimization scheme is applied to reduce the effects of bidirectional disturbances caused by the randomness of RES operation and elastic loads, as well as efficiently solve a different time scale energy scheduling. Simulation results show the effectiveness of the proposed methodology.**

***Index Terms*—Autonomous microgrids, renewable energy sources, two-time scale, hierarchical coordination, demand response management.**

I. Introduction

With an increasing number of smart users, energy scheduling for Autonomous MicroGrids (AMGs) is becoming more challenging due to the time varying power consumption and the random power utilization time. Moreover, with distributed Renewable Energy Sources (RESs) deeply penetrated into AMGs, negative effects related to the intermittent and randomness of RESs, are challenging the way energy has to be managed. Challenges due to energy coordination, including bidirectional disturbances from supply-side and load-side with various operating time scales, have caught more and more interests over the past few years [1].

These disturbances, in addition to low inertial support, can lead to significant fluctuations in power balance. Fast acting Battery Energy Storage Systems (BESSs) can be employed to mitigate such balancing issues [2]–[5]. In [2], an optimization model including battery loss cost is established to obtain a set of optimal parameters of operation strategy in order to realize the economic operation of standalone microgrids. Reference [3] proposes a distributed control strategy for BESS coordination to maintain the supply-demand balance and minimize the total power loss associated with charging/discharging inefficiency. A novel stochastic planning framework is proposed in [4], which determines the optimal BESS capacity and installation cost in isolated MicroGrids (MGs) using a new representation of the BESS energy diagram. A methodology is presented in [5] to minimize the total cost of buying power from different energy producers, which is primarily based on the controlled operation of a BESS in the presence of practical system constraints. However, significant variability from loads and RESs may also cause undesirable cycling in BESSs as these devices will need to charge and discharge frequently to help compensate for such variability. In addition, energy storage may not always be available due to the limits imposed to it. Therefore, proper coordination of AMGs is essential guarantee that RESs are utilized efficiently while ensuring system-wide dynamic balance [6]–[8].

Although AMGs can cooperate with each other, few research works consider their dynamic random fluctuations at the different time scales of supply-side and demand-side simultaneously. The concept of multi-time scale is proposed in [9]–[12]. In [9], a different time-scale dispatch scheme is applied to smooth out the fluctuations of RESs, which focuses on the supply-side. For disturbances caused by the demand-side, a hierarchical control strategy is developed in [10], which solves the problem of peaks and valleys of loads over multiple time scales. Reference [11] proposes an improved multi time-scale co-optimization algorithm for AMG coordinated scheduling to meet customer's demands. The authors of [12] present a multiple-time-scale rolling optimal dispatching framework to cope with the impact of predicted source-load deviations on AMGs. The aforementioned multi-time

Manuscript received July 28, 2019; revised November 4, 2019 and January 22, 2020; accepted February 26, 2020. Date of publication March 16, 2020; date of current version August 21, 2020. This work was supported in part by the National Natural Science Foundation of China under Grant 61873166, Grant 61673275, Grant 61473184, and Grant 61590924, and in part by the China Scholarship Council Foundation. Paper no. TSG-01082-2019. *(Corresponding author: Jing Wu.)*

Yigao Du was with the Department of Energy Resources Engineering, Stanford University, Stanford, CA 94305 USA. He is now with the Department of Automation, Key Laboratory of System Control and Information Processing, Ministry of Education, Shanghai Jiao Tong University, Shanghai 200240, China (e-mail: yigaodu@sjtu.edu.cn).

Jing Wu, Shaoyuan Li, and Chengnian Long are with the Department of Automation, Key Laboratory of System Control and Information Processing, Ministry of Education, Shanghai Jiao Tong University, Shanghai 200240, China (e-mail: jingwu@sjtu.edu.cn; syli@sjtu.edu.cn; longcn@sjtu.edu.cn).

Simona Onori is with the Department of Energy Resources Engineering, Stanford University, Stanford, CA 94305 USA (e-mail: sonori@stanford.edu).

Color versions of one or more of the figures in this article are available online at http://ieeexplore.ieee.org.

Digital Object Identifier 10.1109/TSG.2020.2980873

scale coordinated strategies are centralized or distributed, and mainly focused on the energy management, where the total power production matches the long-term demand. We proposed a novel conditional probability distribution model to characterize the dynamic process of energy dispatch of short-term energy dispatching [13]. However, these strategies are not applicable to the scenario where the demand may exceed the supply. Specifically, the failure of AMGs in load feeding is common in inslanded mode, with impact on the stability and reliability of the whole system [14]–[17].

It should be pointed out that most of the published research focuses on the overall system balance between supply and demand side [18]–[20]. In this paper, a two-time scale and multi-step coordinated control method for AMGs based on a hierarchical coordination framework is proposed for the case that the demand may exceed the supply. This situation is very common in isolated mode since the system is decoupled from the main grid and the supply depends on uncontrollable RESs and limited battery usage, which may not match the demand at all times. A specific characteristic of the proposed architecture is that it is divided into three levels to satisfy their goals to make it easier to manage and operate the system. The main contributions of this paper can be summarized as follows:

1) Our research work investigates the energy management problem where the supply may be less than the demand for the whole system. No assumption is made on the overall supply of AMGs has to match the overall demand. This is reasonable for AMGs since the AMGs are isolated from the main grid, RES and loads have uncontrollable uncertainties. The proposed energy management strategy can deal with the imbalanced energy effectively by shifting or cutting loads based on users' needs.
2) A three-level hierarchical control structure is designed to coordinate the sub control systems, which can reduce the disturbances caused by the randomness of RESs and loads. Different from the standard three-level (top-medium-down) architecture, where the top level optimizes energy dispatch on supply-demand balance scenario, the medium-top-down control structure proposed in this paper is suitable for the energy dispatch on supply-demand imbalance scenario. In fact, the top level may not have enough power to trade among AMGs in autonomous mode while the medium level can coordinate the imbalanced energy initially through the local BESS. In the proposed control structure, the top level is optimized in a second moment, depending on whether there is surplus of energy or not.
3) A two-time scale energy optimization management approach is proposed, where different layers perform over different sampling periods. A slow scale time is used to deal with the top and medium optimization level to achieve the overall system balance in the long-term. Morever, the bottom level optimization problem is established to meet users' demands at a fast scale.

The rest of this paper is organized as follows. AMG design and battery modeling are briefly introduced in Section II. In Section III, we formulate the problem as a hierarchical coordination scheme. Section IV presents the proposed multi-step and two-time scale optimization problem and its solution. Simulation results and discussion are presented in Section V, and conclusions are given in Section VI.

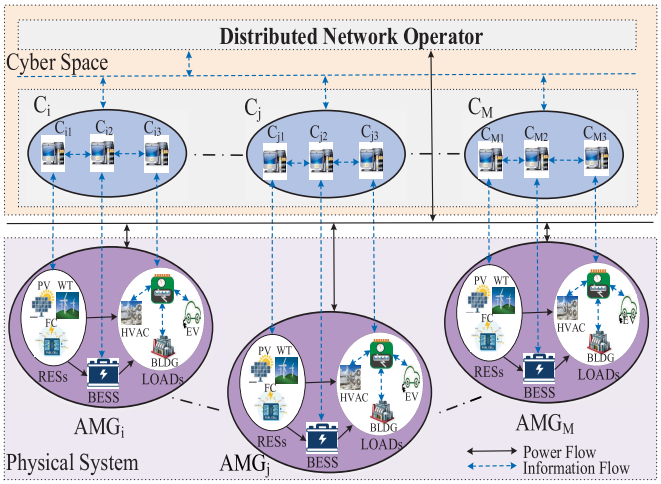

Fig. 1. Schematic of the microgrid systems developed in this paper.

II. AMG Design and Modeling

In this section, we provide detailed modeling of the dynamics of AMG components and their constraints.

A. Description of AMG

A cooperative network of M AMGs is illustrated in Fig. 1. Each microgrid is equipped with RESs (PhotoVoltaics (PV), Wind Turbines (WT) and fuel cells), BESSs and loads. In the case where each microgrid is operated in autonomous mode, the load demand will firstly be supplied by RESs and BESS units locally. Through the advanced metering infrastructure, each microgrid can receive the published data from the Distribution Network Operator (DNO), and have the options to share its own information with DNO. It is assumed that all AMGs are connected to the same DNO and the power exchange can take place in both directions.

It is easy to see that the framework in Fig. 1 is a distributed control architecture, where each AMG has its own controller and shares information with other subsystems. Each AMG achieves energy coordination only through the DNO since no extra power lines are required among AMGs in practical cases. Moreover, the power generation in the network of AMGs is mainly based on RESs.

B. Demand Response Management

Let $P_i^L(k)$ denote the total power demand of users in microgrid $i \in M$ at time k. We classify the loads into two categories [21]: critical loads and elastic loads. The critical loads, such as freezer and illumination demands, can always be met over time. The elastic loads, such as heating, drying, illumination demand and Plug-in Hybrid Electric Vehicles (PHEVs), can be flexibly scheduled over time.

The Demand Response Management (DRM) can only control the elastic loads, and be categorized into time-based and

incentive-based programs [22]. Time-based programs encourage users to adjust their load profiles according to the varying prices of the electricity while the incentive-based ones provide motivated payments for users who reduce electricity use at certain hours [23]. In [24], the difference between initial load $P_i^L(k)$ and responded (curtailed) load $\Delta P_i^L(k)$ can be presented as virtual power generation as follows:

$$P_i^{DR}(k) = P_i^L(k) - \Delta P_i^L(k) \tag{1}$$

For the case that customers prefer comfortable needs rather than curtailing the loads, they have to pay extra price for comfortability. In determining the cost attached to providing Demand Response (DR), incremental marginal cost is proposed to treat the amount of curtailed demand as a virtual generation unit as shown in [25] and [26].

With the consideration of customers' satisfaction request, the cost function of the virtual generation unit, $J_{i,DR}(k)$, is finally defined as below:

$$J_{i,DR}(k) = \frac{1}{2} a_i \Delta P_i^L(k)^2 + b_i \Delta P_i^L(k) \tag{2}$$

where a_i and b_i are independently positive coefficients of curtailed demand vs. discomfort cost.

C. Battery Modeling

Exchange of electric energy in power systems relies heavily on executing the scheduled strategies. Deviations from these schedules lead to an imbalance between supply and demand and are usually penalized by the regulator. BESSs can be used to compensate imbalances arising from uncontrollable loads and generators and thereby minimize imbalance penalties. Meanwhile, the actual operation of a battery system leads to a decline of life time in terms of allowable charging/discharging rate [27]–[29].

We denote $E_i(k)$ as the energy stored in the BESS of microgrid i, with the associated piece-wise affine (PWA) LTI representation [6] being

$$E_i(k+1) = \begin{cases} E_i(k) + \eta_i^{ch} P_i^{BESS}(k), & P_i^{BESS}(k) > 0 \\ E_i(k) + 1/\eta_i^{dch} P_i^{BESS}(k), & P_i^{BESS}(k) < 0 \end{cases} \tag{3}$$

where $P_i^{BESS}(k)$ is the overall power mismatch for microgrid i at time k defined as [30]:

$$P_i^{BESS}(k) = P_i^{RES}(k) - P_i^L(k) \tag{4}$$

where $P_i^{BESS}(k) > 0$ and $P_i^{BESS}(k) < 0$ means BESS charging and discharging, respectively. $\eta_i^{ch/dch}$ is the charging/discharging efficiency. $P_i^{RES}(k)$ is total renewable energy generated by microgrid i at time k.

In this study, we assume that the BESS can only be either charged or discharged during the whole period. In order to penalize the high charging rate and high discharging rate of BESS, the following cost function is proposed

$$J_{i,bat}(k) = P_i^{BESS}(k)^2 \tag{5}$$

D. Constraints

The proposed model is restricted by some constraints, classified as follows:

Constraint 1: demand response constraints

$$\underline{P}_i^L \le P_i^L(k) \le \overline{P}_i^L, \forall i \in M \tag{6}$$

$$0 \le \Delta P_i^L(k) \le \Delta \overline{P}_i^L, \forall i \in M \tag{7}$$

where $\underline{P}_i^L$ is the minimum active power of total demand; $\overline{P}_i^L$ is the maximum active power of total demand, which should be smaller than the electrical line power to satisfy the power flow constraint, and $\Delta \overline{P}_i^L$ is the maximum energy dispatch of controllable loads.

Constraint 2: battery limits

$$0 \le E_i(k) \le \overline{E}_i, \forall i \in M \tag{8}$$

$$\underline{P}_i^{BESS} \le P_i^{BESS}(k) \le \overline{P}_i^{BESS}, \forall i \in M \tag{9}$$

where $\overline{E}_i$ is the upper bound of stored energy in microgrid i. $\underline{P}_i^{BESS}$ and $\overline{P}_i^{BESS}$ denote the minimum and maximum charging/discharging limits of the BESS, respectively.

Constraint 3: renewable power limits

$$0 \le P_i^{RES}(k) \le \overline{P}_i^{RES}, \forall i \in M \tag{10}$$

where $\overline{P}_i^{RES}$ is the maximum output power produced by the renewable source, which is limited by the total capacity of electrical lines. The implementation of RESs in the AMG gives EMS a more cumbersome task to track the instantaneous supply/demand balance. RESs are considered to have a great variation due to natural processes such as storms and clouds. Hence, we assume that the RESs in each AMG operate between its minimum and maximum power output limits.

III. Problem Formulation

A. Control Architecture

We consider a setup as depicted in Fig. 1. The operation of each AMG aims to satisfy supply-demand balance and meanwhile to minimize the operational cost. To address the uncertainties arisen by RESs and load demands, a hierarchical control framework is developed in this paper, which includes three levels as shown in Fig. 2.

In the top level, DNO can be regarded as a higher-level autonomous control, who is responsible for maintaining the system-wide supply-demand balance. In addition, from the behavior of each AMG, DNO decides the energy exchange with the AMGs. This can be considered as a global control objective, which has to be achieved through the operation of all entities. The medium level focuses on local AMGs and various controllers may perform several tasks independently. The objective of each local AMG is to coordinate operation of different energy modules and supply the demanded energy to users. The bottom level is managed by the aggregator, which is introduced to compensate the deviations between supply and demand from upper level schedules. Each aggregator manages all of elastic users in each AMG to realize a hierarchical control architecture for those users.

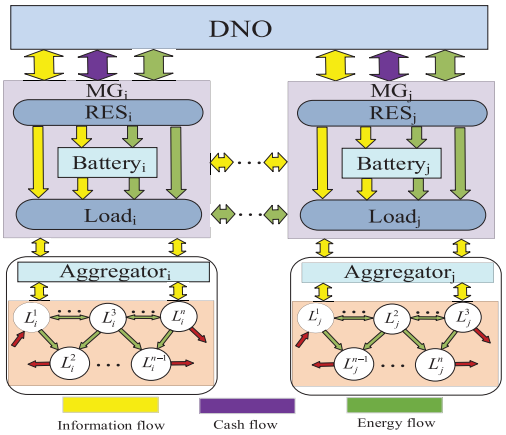

Fig. 2. Hierarchical coordinated energy management architecture.

B. Hierarchical Optimization

In practical scenarios, the energy coordination layer and the load dispatching layer are performed with different sampling periods in the AMG. Morever, there also exists information exchange between different layers in both directions. A two-time scale control strategy is adopted to solve the different time scale scheduling problem. Three optimization problems have been formulated. Given that the demand may exceed the supply among the whole system, the DNO may not have enough power to trade with AMGs. Hence, the optimization in the medium level is firstly solved in the slow time scale framework. Based on the load demands, RESs prediction information, and BESS charge/discharge, the power exchanged between each individual AMGs and DNO and the energy dispatched within an aggregator are optimized. If critical loads' requests cannot be satisfied or surplus of RESs can be provided to DNO, the imbalance information of local AMGs will be uploaded to the DNO. Secondly, the optimization problem in the top layer will coordinate energy exchange between DNO and AMGs at the same rate as that the medium layer. The optimal allocation to users are deduced and transferred to the bottom layer as the constraints for the third optimization problem. Finally, the third optimization is realized in the bottom layer. The aggregator optimizes energy allocation to users at a fast scale sampling period.

IV. Two-Time Scale and Multi-Step Optimization

The multi-step optimization for the two-time scale problem is formed by three parts: the self-scheduling in the medium level is to coordinate several types of energy requests at a slow time scale; rescheduling in the top level determines its decision making based on the each reaction of AMGs at a slow time scale; DRM in bottom layer is implemented to manage dispatchable loads at a fast time scale. For any subsystem $i = 1, 2, \ldots, M$, the notation $(\cdot)_i(k+l|k)$ is used to represent the predicted data at time instant $k+l, l \geq 0$, based on data at time k.

A. Step 1: Local Optimization

1) Objective Function: The main objective of the medium layer is to achieve peak shaving and load shifting within the customer satisfaction as follows:

$$\Phi_{1i} = \sum_{l_s=1}^{N_s} \Big(\xi_{i1} J_{i,bat}(k+l_s|k) + \xi_{i2} J_{i,DR}(k+l_s|k)\Big) + \xi_{i3}\lambda_i(k)\Big(P_i^B(k+l_s|k) - P_i^S(k+l_s|k)\Big)^2 \quad (11)$$

where N_s is the energy scheduling period (24 hours in one day) and l_s is the slow time interval, $\xi_{ij}, i = 1, \ldots, M, j = 1, \ldots, 3$ are weighted coefficients, $\lambda_i(k)$ is the price of exchanged power at time k and is represented by the actual electrical price, which is related to the type of AMG and the relevant government policy. In (11), $P_i^B(k+l_s|k)$ is the power purchased from DNO, and $P_i^S(k+l_s|k)$ is the power sold back to DNO.

The first term in the objective function is related to scheduling the BESS to maintain the local balance between supply and demand in the AMG, while the second term is related to minimizing discomfort costs of controllable loads. The last term characterizes the optimized amount of purchased energy from DNO. Thus, *Problem 1* can be written as

$$\min_{U_i(k+l_s|k)} \Phi_{1i} \quad (12)$$

where $U_i(k+l_s|k) \in \Omega_i$ is the vector of decision variables as follows

$$U_i(k+l_s|k) = \Big[\Delta P_i^L(k+l_s|k) \quad P_i^B(k+l_s|k) \quad P_i^S(k+l_s|k)\Big]^T \quad (13)$$

and Ω_i is the set of admissible controls for subsystem i, $\Delta P_i^L(k+l_s|k)$ is the adjustment for power dispatch of aggregator, $P_i^B(k+l_s|k)$ is the power purchased from DNO, $P_i^S(k+l_s|k)$ is the power sold back to DNO for system i. The solution to *Problem 1* is denoted by $\mathbf{U}_i^{*(p)}$ and $\mathbf{U}_i^{*(p)} = [U_i^{*(p)}(k|k), U_i^{*(p)}(k+1|k), \ldots, U_i^{*(p)}(k+N_s-1|k)]^T$.

2) Constraints: The power balance and some physical limitations of the devices in the ith AMG, such as trading power limitation of each microgrid and total capacity limitation of electrical lines, must be satisfied with the local objective function. The electricity purchased (sold) from (to) DNO is bounded as

$$0 \leq P_i^B(k+l_s|k) \leq \overline{P}_i^B, 0 \leq P_i^S(k+l_s|k) \leq \overline{P}_i^S, \quad (14)$$

The other constraints in the medium level layer are (1), (3)–(4), (6)–(10).

B. Step 2: DNO Optimization (Rescheduling)

In the proposed framework, DNO is considered as a common coupling node which trades energy with AMGs. It receives imbalanced energy information from each AMG and determines an optimal trajectory for each AMG. As a higher-level autonomous entity, DNO makes a strategic decision to guarantee each AMG's profit and satisfactory. At each control cycle, AMGs will send its own request and follow the optimal trajectory that DNO returns. AMGs are the ones that seek to satisfy their customers with certain comfortable level and maximum revenue. DNO guarantees that the requests from AMGs are mostly fulfilled according to priority and bid rule.

By doing so, local AMGs can meet the demand of their loads in an economical manner with high user satisfaction.

1) Objective Function: To formulate the DNO optimization problem, the cost of power exchange from the medium layer is considered. The DNO's objective function can be formulated as

$$\Phi_2 = \sum_{l_s=1}^{N_s}\left(\left(\sum_{i=1}^{M}\lambda_i(k)\left(P_i^B(k+l_s|k) - P_i^S(k+l_s|k)\right)^2\right) + \lambda(k)\left(P_{DNO}^B(k+l_s|k) - P_{DNO}^S(k+l_s|k)\right)^2\right) \tag{15}$$

where $\lambda(k)$ is the average price of AMGs over the optimization horizon defined as follows

$$\lambda(k) = \frac{\sum_{i=1}^{M}\lambda_i(k)}{M} \tag{16}$$

and $P_{DNO}^B(k+l_s|k)$ is the power purchased by DNO from AMGs, and $P_{DNO}^S(k+l_s|k)$ is the power sold by DNO to AMGs. Thus *Problem 2* can be written as

$$\min_{U_i(k+l_s|k)} \Phi_2 \tag{17}$$

where $U_i(k+l_s|k)$ is given in (13).

2) Constraints: The model includes equality and inequality constraints.

The power exchange balance between DNO and AMGs must be satisfied. Related equality constraints are as follows:

$$\sum_{i=1}^{M} P_i^B(k+l_s|k) = P_{DNO}^S(k+l_s|k) \tag{18}$$

$$\sum_{i=1}^{M} P_i^S(k+l_s|k) = P_{DNO}^B(k+l_s|k) \tag{19}$$

$$\sum_{i=1}^{M} P_i^B(k+l_s|k) = \sum_{i=1}^{M} P_i^S(k+l_s|k) \tag{20}$$

In our settings, critical loads of the whole system can always be met even though local critical loads of individual AMG may not be satisfied. Hence, (21) is necessary to describe this assumption.

$$\sum_{i=1}^{M}\left(P_i^{RES}(k+l_s|k) + E_i(k+l_s|k)\right) \geq \sum_{i=1}^{M} P_i^{DR}(k+l_s|k) \tag{21}$$

In addition, inequality constraints are the same as those for the medium level model, which are (6)–(10), (14).

C. Step 3: Aggregator Optimization

By solving the above optimization problem, we can obtain the optimal solution $U_i^*(k+l_s|k)$, that is the optimal adjustment for power dispatch of aggregator $\Delta P_i^{L*}(k+l_s|k)$, power purchased from DNO $P_i^{B*}(k+l_s|k)$ and power sold back to DNO $P_i^{S*}(k+l_s|k)$. Based on the optimal information in the upper level, the aggregator of each AMG optimizes power allocation to users at a fast time scale in the bottom level. According to (1), the optimal power of the aggregator $P_i^{DR*}(k+l_s|k)$ is:

$$P_i^{DR*}(k+l_s|k) = P_i^L(k+l_s|k) - \Delta P_i^{L*}(k+l_s|k) \tag{22}$$

Since the upper layer and bottom layer are optimized on a different sampling scheme, we set

$$U_i^*\left(k+l_s+nl_f|k\right) = U_i^*(k+l_s|k), \quad n = 0,\ldots,\left(\left(l_s/l_f\right)-1\right) \tag{23}$$

where l_f is the fast sampling period.

1) Objective Function: The objective of the aggregator is to optimize energy allocation to users so that the real-time supply and optimal energy allocation can be satisfied in the short-term as follows:

$$\Phi_{3i} = \sum_{n=1}^{(l_s/l_f)-1}\left(\eta_{i1}\left(\Delta P_i^L\left(k+l_s+nl_f|k\right)\right)^2 + \eta_{i2}\left(P_i^{DR}\left(k+l_s+nl_f|k\right) - P_i^{DR*}(k+l_s|k)\right)^2\right) \tag{24}$$

where $\eta_{ij}, i = 1,\ldots,M, j = 1,\ldots,2$ are weighted coefficients.

The first term in the objective index is related to the minimization of the operational cost to adjust for the controllable loads while the second term is to track the optimal trajectory $P_i^{DR*}(k+l_s|k)$ from upper layer. Thus *Problem 3* can be written as

$$\min_{z_i\left(k+l_s+nl_f|k\right)} \Phi_{3i} \tag{25}$$

where the decision variable $z_i(k+l_s+nl_f|k) \in \Omega_i$ for *Problem 3* is chosen such that

$$z_i\left(k+l_s+nl_f|k\right) = \left[\Delta P_i^L\left(k+l_s+nl_f|k\right)\right]^T \tag{26}$$

The solution to *Problem 3* is denoted by $\mathbf{z}_i^{*(p)} = [z_i^{*(p)}(k|k), z_i^{*(p)}(k+l_s+l_f|k), \ldots, z_i^{*(p)}(k+(l_s/l_f)-2|k)]^T$.

2) Constraints: The problem constraints are related to the demand response. So all constraints in the bottom level model are (1), (6)−(7), (22).

D. Two-Time Scale Hierarchical MPC Algorithm

As discussed earlier, we accept the optimal information from upper layer $P_i^{DR*}(k+l_s|k)$ and allocate the energy to users to satisfy the demand in real time. In this framework, the top layer DNO controller and medium layer are executed periodically every l_s time intervals (a scheduling cycle), while the bottom layer aggregator controller is executed every l_f time intervals equivalent to the duration of a control cycle. Let p represent the number of allowable iterations for the sampling interval.

In this way, at the beginning of each scheduling cycle, local AMG will first shift the load by solving a *Problem 1*. The computed information that the local AMG has surplus/deficient of energy is then sent to DNO. DNO schedules the energy among AMGs by solving *Problem 2*. Algorithm 1 describes the proposed slow-time scale hierarchical coordination algorithm.

Algorithm 1 Slow-Time Scale Hierarchical Coordination Algorithm

Initialization $E_i(0)$, $P_i^{RES}(0)$, $P_i^L(0)$, $P_i^B(0)$, $P_i^S(0)$, and $\Delta P_i^L(0)$, $\forall i = 1, \ldots, M$
for $k = 1$ **do**
  Receive $\sum_{i=1}^{M} P_i^{BESS}(k)$ from the DNO controller, measure $E_i(k)$, $P_i^{RES}(k)$ and $P_i^L(k)$ at local controller; update the distributional forecasts $P_i^{RES}(k+l_s|k)$, $P_i^L(k+l_s|k)$, $P_i^B(k+l_s|k)$, $P_i^S(k+l_s|k)$ and $\Delta P_i^L(k+l_s|k)$.
  if $P_i^{BESS}(k+l_s|k) < 0$ and $P_i^{RES}(k+l_s|k)+E_i(k+l_s|k) \geq P_i^{DR}(k+l_s|k)$ **then**
    while $\rho_i > \epsilon$ and $p \leq p_{max}$ **do**
      $\mathbf{U}_i^{*(p)} = arg(Problem\ 1), \forall i = 1, 2, \ldots, M.$
      for $\forall i = 1, 2, \ldots, M$ **do**
        $\mathbf{U}_i^p \leftarrow w_i \mathbf{U}_i^{*(p)} + (1 - w_i)\mathbf{U}_i^{p-1}$
        $\rho_i \leftarrow \|\mathbf{U}_i^p - \mathbf{U}_i^{p-1}\|$.
      end for
      $p \leftarrow p + 1$ and go to step 5.
    end while
  else
    while $\rho_i > \epsilon$ and $p \leq p_{max}$ **do**
      $\mathbf{U}_i^{*(p)} = arg(Problem\ 2), \forall i = 1, 2, \ldots, M.$
      for $\forall i = 1, 2, \ldots, M$ **do**
        $\mathbf{U}_i^p \leftarrow w_i \mathbf{U}_i^{*(p)} + (1 - w_i)\mathbf{U}_i^{p-1}$
        $\rho_i \leftarrow \|\mathbf{U}_i^p - \mathbf{U}_i^{p-1}\|$.
      end for
      $p \leftarrow p + 1$ and go to step 14.
    end while
    Send the optimal control sequence $U_i^*(k+l_s|k)$ to the load aggregator.
  end if
  $k \leftarrow k + 1$ and go to step 2.
end for

In each control cycle, the aggregator controller receives the optimal control command $P_i^{DR*}(k + l_s|k)$ and cut the real-time loads by solving *Problem 3*. The proposed fast-time scale DRM algorithm is presented in Algorithm 2.

E. Convergence of the Proposed Algorithm

Theorem 1: If Φ_{1i} satisfies the form in (11), then Φ_{1i} is convex over the set Ω_i.

Proof: From (11), we have $\Phi_{1i} \geq 0$. Rewriting the objective function in (11) based on the distributed discrete-time system model, we have

$$\Phi_{1i} = \sum_{l_s=1}^{N_s} \Big(U_i(k + l_s|k)^T S_1 U_i(k + l_s|k) + S_2 U_i(k + l_s|k) + S_3 \Big) \geq 0 \quad (27)$$

where

$$S_1 = \begin{bmatrix} \frac{1}{2} a_i \xi_{i2} & & \\ & \xi_{i3}\lambda_i(k) & \\ & & \xi_{i3}\lambda_i(k) \end{bmatrix} \geq 0,$$

Algorithm 2 Fast-Time Scale DRM Algorithm

Initialization $P_i^L(k + l_s)$ and $\Delta P_i^L(k + l_s)$, $\forall i = 1, \ldots, M$
Receive the optimal control sequence $U_i^*(k + l_s|k)$.
while $n \leq (l_s/l_f) - 1$ **do**
  Get the estimation of $P_i^L(k + l_s + nl_f|k)$ and $\Delta P_i^L(k + l_s + nl_f|k)$.
  while $\rho_i > \epsilon$ and $p \leq p_{max}$ **do**
    $\mathbf{z}_i^{*(p)} = arg(Problem\ 3), \forall i = 1, 2, \ldots, M.$
    for $\forall i = 1, 2, \ldots, M$ **do**
      $\mathbf{z}_i^p \leftarrow w_i \mathbf{z}_i^{*(p)} + (1 - w_i)\mathbf{z}_i^{p-1}$
      $\rho_i \leftarrow \|\mathbf{z}_i^p - \mathbf{z}_i^{p-1}\|$.
    end for
    $p \leftarrow p + 1$ and go to step 5.
  end while
  Implement the optimal control solution $\Delta P_i^{L*}(k + l_s + nl_f|k)$, shift the corresponding loads.
  $n \leftarrow n + 1$ and go to step 3.
end while

$$S_2 = \begin{bmatrix} b_i \xi_{i2} & & \\ & 0 & \\ & & 0 \end{bmatrix} \geq 0,$$
$$S_3 = \xi_{i1} P_i^{BESS}(k)^2 \geq 0.$$

If we take the second derivative of (27), then

$$\Phi_{1i} = 2N_s \left(\frac{1}{2} a_i \xi_{i2} + 2\xi_{i3}\lambda_i(k) \right) \geq 0$$

Thus, Φ_{1i} is convex. ∎

Theorem 2: If Φ_2 satisfies the form in (15), then Φ_2 is convex over the set Ω_i.

Proof: From (15), we have $\Phi_2 \geq 0$. Rewriting the objective function in (15) based on the distributed discrete-time system model, we have

$$\Phi_2 = \sum_{l_s=1}^{N_s} \left(\left(\sum_{i=1}^{M} U_i(k + l_s|k)^T S_4 U_i(k + l_s|k) \right) + S_5 \right) \geq 0 \quad (28)$$

where

$$S_4 = \begin{bmatrix} 0 & & \\ & \lambda_i(k) & \\ & & \lambda_i(k) \end{bmatrix} \geq 0,$$
$$S_5 = \lambda(k) \Big(P_{DNO}^B(k + l_s|k) - P_{DNO}^S(k + l_s|k) \Big)^2 \geq 0.$$

If we take the second derivative of equation (28), then

$$\Phi_2 = 4N_s \sum_{i=1}^{M} \lambda_i(k) \geq 0$$

Thus, Φ_2 is convex. ∎

Theorem 3: If Φ_{3i} satisfies the form in (24), then Φ_{3i} is convex over the set Ω_i.

Proof: From (24), we have $\Phi_{3i} \geq 0$. Rewriting the objective function in (24) based on the distributed discrete-time system

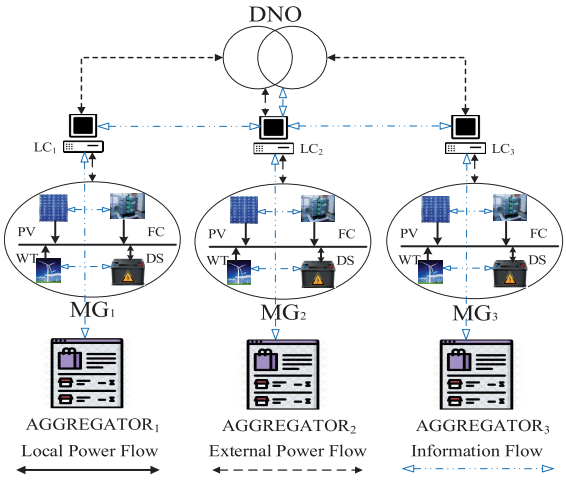

Fig. 3. Schematic of the studied microgrids.

model, we have

$$\Phi_{3i} = \sum_{n=1}^{(l_s/l_f)-1} \Big(z_i\big(k+l_s+nl_f|k\big)^T S_6 z_i\big(k+l_s+nl_f|k\big) - S_7 z_i\big(k+l_s+nl_f|k\big) + S_8 \Big) \geq 0 \quad (29)$$

where

$$S_6 = \eta_{i1} + \eta_{i2} \geq 0,$$
$$S_7 = 2\big(P_i^L\big(k+l_s+nl_f|k\big) - P_i^{DR*}(k+l_s|k)\big) \geq 0,$$
$$S_8 = \big(P_i^L\big(k+l_s+nl_f|k\big) - P_i^{DR*}(k+l_s|k)\big)^2 \geq 0.$$

If we take the second derivative of equation (29), then

$$\Phi_{3i} = 2\big(\big(l_s/l_f\big) - 1\big)(\eta_{i1} + \eta_{i2}) \geq 0$$

Thus, Φ_{3i} is convex. ■

From Theorems 1, 2 and 3, $\Phi_{1i}, \Phi_2, \Phi_{3i}$ are convex and bounded from below. Using [31, Lemma 1], the sequence of cost functions $\Phi_{1i}(\mathbf{U}_i^p)$ and $\Phi_2(\mathbf{U}_i^p)$ generated by Algorithm 1, and $\Phi_{3i}(\mathbf{z}_i^p)$ generated by Algorithm 2 are non-increasing with iteration number p. Hence, the proposed algorithms are convergent based on the above conditions. The detailed proof is similar to [31, Lemmas 1 and 2]. For simplicity, the proof is omitted.

V. Case Study

The structure of system analyzed in this paper is illustrated in Fig. 3. The considered radial distribution network includes three AMGs which are equipped with PV, WT, fuel cells, battery and local loads. In the test system, AMG 1, AMG 2 and AMG 3 are connected to the network via black dashed lines. The connection line between DNO and AMGs is shown via double headed arrows. In addition, to express the possibility of exchange the information between AMGs, blue dashed lines via double headed arrows accessed to connect the AMGs. To simplify the mathematical discussion, the power and energy were converted to power unit (p.u.). We use an MPC control horizon of $N_s = 24$, which corresponds to one hour intervals over a 24 hour period. The slow sampling period l_s of local AMGs and DNO optimization are set by 1 h; the fast sampling period l_f of aggregator optimization is set to 15 min.

TABLE I
Initial Conditions Used in Simulations

AMGs	$P_i^{RES}(0)$	$P_i^L(0)$	$P_i^B(0)$	$P_i^S(0)$	$\Delta P_i^L(0)$
AMG_1	25	20	0	0	0
AMG_2	10	18	0	0	0
AMG_3	20	28	0	0	0

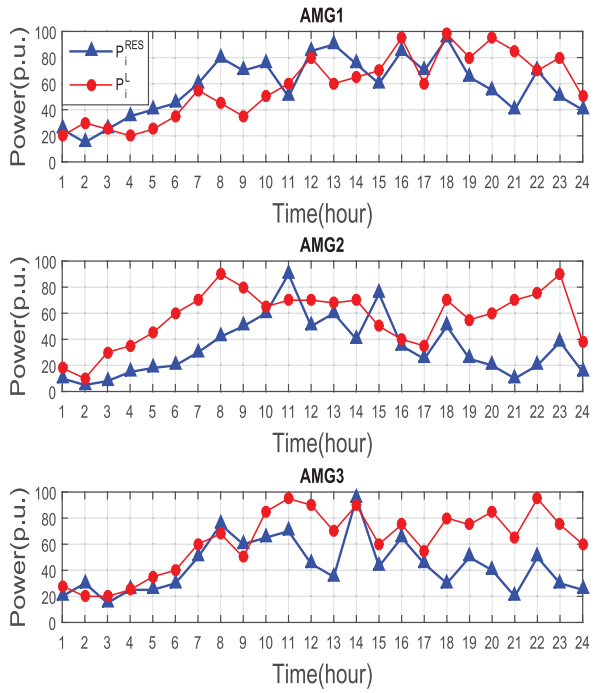

Fig. 4. Profiles of the RESs and loads of AMGs.

A. Simulation Setup

Set the minimum active power of total demand $\underline{P}_i^L$ to 10 p.u., and $\overline{P}_i^L = 100$ p.u., $\Delta\overline{P}_i^L = 70$ p.u., $\forall i = 1, 2, 3$. The maximum power of RESs are 100 p.u. The initial energy values of the three batteries are set to $E_1(0) = 30, E_1(0) = 20, E_1(0) = 50$ p.u., $\underline{P}_i^{BESS}$, $\overline{P}_i^{BESS}$, $\overline{E}_i$ are chosen to be -30 p.u., 30 p.u., 50 p.u., respectively, and $\eta_i^{ch} = 0.7$, $\eta_i^{dch} = 0.65$, $\forall i = 1, 2, 3$. The initial conditions of other variables are shown in Table I. Also, the upper bound of buying/selling electricity from/to DNO is set $\overline{P}_i^B = 30$ p.u. and $\overline{P}_i^S = 30$ p.u., respectively. Let the cost weight coefficients be $\xi_{i1} = 0.8, \xi_{i2} = 0.1, \xi_{i3} = 0.1$, $\eta_{i1} = 0.6, \eta_{i2} = 0.4$ and $\gamma_{i1} = 0.3, \gamma_{i2} = 0.7$.

B. Results and Discussion

Along with the data provided in Section V-A, realistic data of both the load demands and RESs output profiles are needed, as well as the market electricity prices. These are shown in Figs. 4, 5 and 6. Fig. 4 gives the profiles for the RESs and

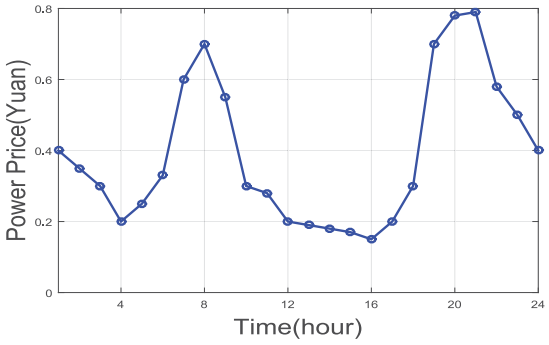

Fig. 5. Market electricity price in China.

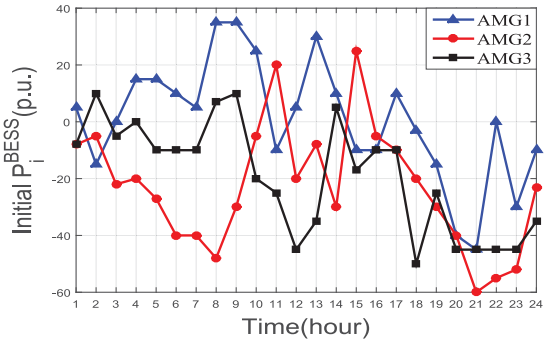

Fig. 6. Imbalanced energy profiles of AMGs.

loads of the three AMGs during a 24 h period, while Fig. 5 collects the unitary trading prices between DNO and AMGs. From Fig. 4, we can see that during 7-9, AMG 1 has surplus power to DNO since RESs are higher than the load demand. However, AMG 2 needs to buy some power from DNO since the load demand is bigger than RESs supply while the supply-demand in AMG 3 is nearly balanced. Fig. 5 indicates how the price for trading energy is dependent or responds to the surplus/deficit energy accordingly. It is forecasted according to generation price, customers' satisfaction and battery's charging/discharging cost. When there is a deficit, the market price is increased due to the scarce resources and will fluctuate according to AMGs' decision. For example, during the 12-17 time window, the price is as low as 0.2 Yuan because there is surplus of RESs to supply the loads among AMGs. On the other hand, the price during 20-21 is as high as 0.8 Yuan due to a RES deficit at night.

Fig. 6 presents the imbalanced energy of each AMGs, where positive values indicate that the AMG has a surplus of energy, and negative values indicate that there is deficit in energy request. It is easy to see that during daytime, AMG 1 has energy surplus while AMG 2 has energy shortage. At night, there exists energy deficit in all of AMGs because of shortage of RESs. Especially during the time interval 3-14, the power generation of renewable energy of AMG 1 has a surplus in power while AMGs 2 and 3 need power. Thus, those AMGs must apply the proposed method to support the loads.

1) Results of Step 1: The local optimization results for each AMG, which are determined by the medium level, are given in Fig. 7 and Fig. 8. The corresponding results of the control action are then sent to the upper layer DNO and lower layer aggregator. Fig. 7 presents charging/discharging profiles

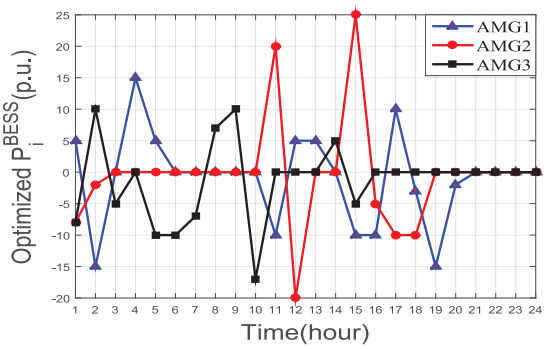

Fig. 7. Battery charging/discharging signals for AMGs in response to DRM.

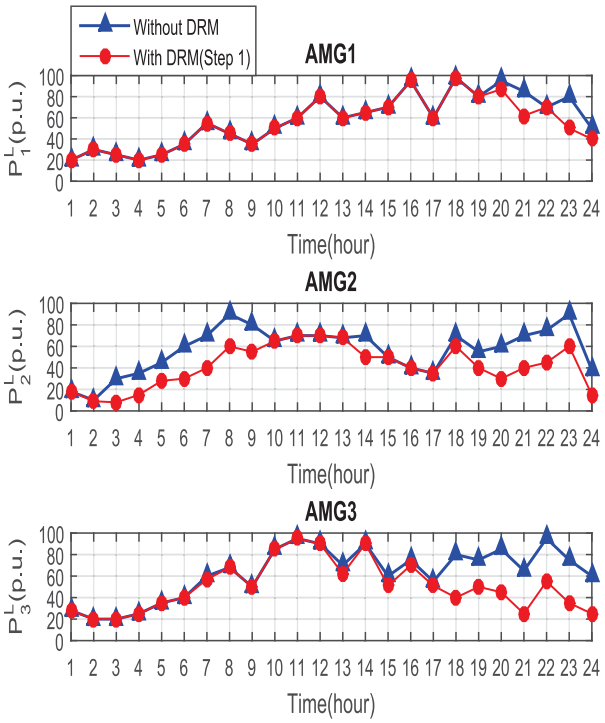

Fig. 8. Load profiles of AMGs in response to DRM.

of BESS in one day. The figure illustrates that the BESS of each AMG can be operated in their limited range, varying from −25 p.u. to 25 p.u.. For example, AMG 1 can charge the local BESS at 4am because the supply is larger than the demand. The BESS cannot be discharged at 21-24 because the capacity has reached the lower bound limit. Fig. 8 displays the optimal energy management of each AMG before/after load shifting in response to their own DR, e.g., the load with DRM has been shifted accordingly during 19-24 since RESs in AMG 1 are not sufficient for the load in Fig. 4. Similarly, the load in AMG 2 and AMG 3 have been shifted, respectively.

2) Results of Step 2: After receiving the requested information from the local AMG, the DNO scheduling is implemented according to the overall surplus energy of the whole system, which is reported in Fig. 9. A positive value indicates that the energy has been purchased by the local AMG from DNO. A negative value indicates that AMG has sold such amount of energy to DNO. For example, at 7, AMG 2 purchases 10 p.u. from DNO and AMG 1 sells 5 p.u. to DNO,

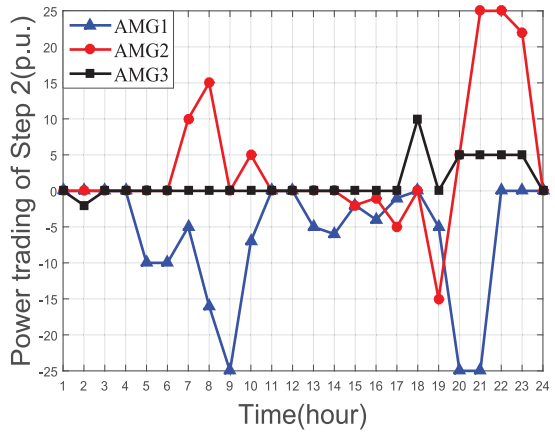

Fig. 9. Trading power in DNO optimization.

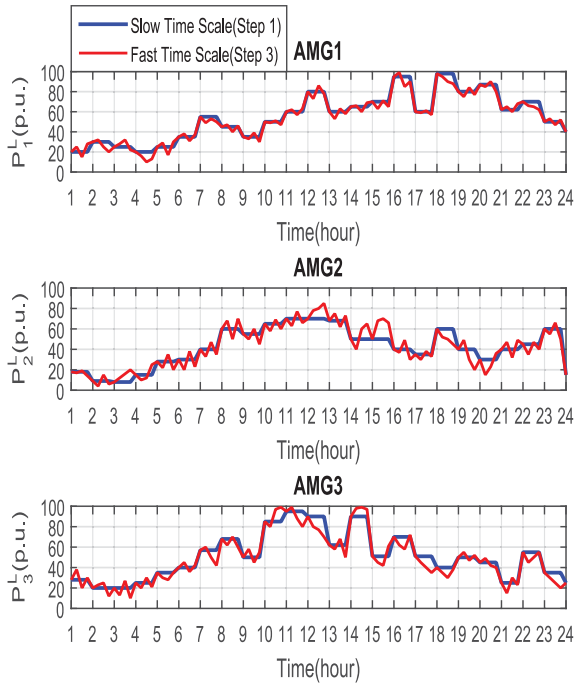

Fig. 10. DR in Aggregator optimization.

while there is no trading in AMG 3. This indicates that there is still supply-demand imbalance among AMGs. Next, the aggregator optimization is executed. Those information will be sent to Step 3 optimization for load shedding.

3) Results of Step 3: The hourly optimization done at Step 1 and 2 can achieve effective utilization of energy in the long term. Thus, the optimal solution is sent to the load aggregator for execution. At the bottom layer, the balance between supply and demand can be achieved in the short term, as illustrated in Fig. 10. Compared with no demand response strategy, the total amount of load shedding in the whole system is 723 p.u. during one day. It is clear that real time optimization at a fast-time scale can be tracked by the optimized curves at a slow-time scale.

In order to assess the level of RESs effficiency utilization, we define the Energy Balance Ratio (*EBR*) as

$$EBR = \frac{\sum_{i=1}^{M} P_i^{ES}(k)}{\sum_{i=1}^{M} P_i^{DR}(k)}, \tag{30}$$

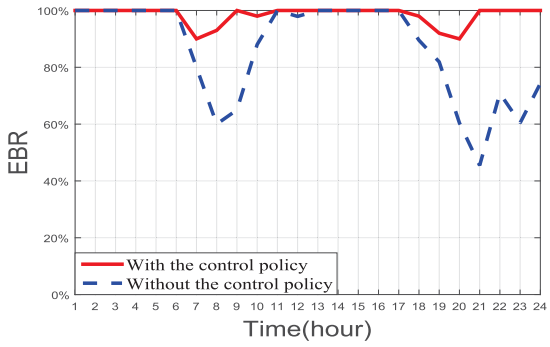

Fig. 11. Comparison of EBR utilization.

where $P_i^{ES}(k)$ denotes total power supply at time instant k as follow

$$P_i^{ES}(k) = P_i^{RES}(k) + P_i^{BESS}(k) + P_i^{B}(k) - P_i^{S}(k) \tag{31}$$

In Fig. 11, we can see that the EBR with our proposed control method is above 90% during all times. From 11 to 14, both lines are also flat because local AMGs can be self-sufficient. However, as can be seen from simulation results, there are a lot more differences when there are no solar sources from 19 to 24.

VI. Conclusion

This paper provides a new hierarchical scheme for the coordinated energy management of AMGs. Due to different control layers implemented with different sampling periods, the optimization problem for each layer accounts for the disturbances in both supply and demand sides. At the slow scale, the proposed decision-making process seeks to minimize the operational cost of AMG owners in the long term taking into account the minimization of the DNO's trading costs. AMG owners schedule their RESs, BESS and load consumptions to achieve the local balance in the medium layer. On the other hand, DNO participates in the energy market and is associated with AMGs in the top layer, and interacts with AMG owners to feed electrical loads implementing demand response program during the scheduling horizon. At the fast scale, the energy balance between supply and demand of smart users can be realized in the short-term. Simulation studies demonstrate that the proposed control scheme can be utilized at different layers for multi-step decision-making objectives. Future work will focus on including technical constraints such as reactive power and thermal limits for AMGs, as well as the extension of the proposed framework to active distribution system.

References

[1] E. Mayhorn, L. Xie, and K. Butler-Purry, "Multi-time scale coordination of distributed energy resources in isolated power systems," *IEEE Trans. Smart Grid*, vol. 8, no. 2, pp. 998–1005, Mar. 2017.

[2] B. Zhao, X. Zhang, J. Chen, C. Wang, and L. Guo, "Operation optimization of standalone microgrids considering lifetime characteristics of battery energy storage system," *IEEE Trans. Sustain. Energy*, vol. 4, no. 4, pp. 934–943, Oct. 2013.

[3] Y. Xu, W. Zhang, G. Hug, S. Kar, and Z. Li, "Cooperative control of distributed energy storage systems in a microgrid," *IEEE Trans. Smart Grid*, vol. 6, no. 1, pp. 238–248, Jan. 2015.

[4] H. Alharbi and K. Bhattacharya, "Stochastic optimal planning of battery energy storage systems for isolated microgrids," *IEEE Trans. Sustain. Energy*, vol. 9, no. 1, pp. 211–227, Jan. 2018.

[5] M. Khalid, A. Ahmadi, A. V. Savkin, and V. G. Agelidis, "Minimizing the energy cost for microgrids integrated with renewable energy resources and conventional generation using controlled battery energy storage," *Renew. Energy*, vol. 97, pp. 646–655, Nov. 2016.

[6] Y. Du, J. Wu, S. Li, C. Long, and I. C. Paschalidis, "Distributed MPC for coordinated energy efficiency utilization in microgrid systems," *IEEE Trans. Smart Grid*, vol. 10, no. 2, pp. 1781–1790, Mar. 2019.

[7] Y. Du, J. Wu, S. Li, and C. Long, "Enhanced distributed MPC design for efficiency utility of autonomous multi-microgrids," in *Proc. 11th Asian Control Conf. (ASCC)*, Gold Coast, QLD, Australia, 2017, pp. 829–834.

[8] M. Jalali, K. Zare, and H. Seyedi, "Strategic decision-making of distribution network operator with multi-microgrids considering demand response program," *Energy*, vol. 141, pp. 1059–1071, Dec. 2017.

[9] Z. Bao, Q. Zhou, Z. Yang, Q. Yang, L. Xu, and T. Wu, "A multi time-scale and multi energy-type coordinated microgrid scheduling solution—Part I: Model and methodology," *IEEE Trans. Power Syst.*, vol. 30, no. 5, pp. 2257–2266, Sep. 2015.

[10] Z. Zhao, P. Yang, J. M. Guerrero, Z. Xu, and T. C. Green, "Multiple-time-scales hierarchical frequency stability control strategy of medium-voltage isolated microgrid," *IEEE Trans. Power Electron.*, vol. 31, no. 8, pp. 5974–5991, Aug. 2016.

[11] Z. Bao, Q. Zhou, Z. Yang, Q. Yang, L. Xu, and T. Wu, "A multi time-scale and multi energy-type coordinated microgrid scheduling solution—Part II: Optimization algorithm and case studies," *IEEE Trans. Power Syst.*, vol. 30, no. 5, pp. 2267–2277, Sep. 2015.

[12] H. Qiu, W. Gu, Y. Xu, and B. Zhao, "Multi-time-scale rolling optimal dispatch for AC/DC hybrid microgrids with day-ahead distributionally robust scheduling," *IEEE Trans. Sustain. Energy*, vol. 10, no. 4, pp. 1653–1663, Oct. 2018.

[13] Y. Du, J. Wu, S. Li, C. Long, and S. Onori, "Coordinated energy dispatch of autonomous microgrids with distributed MPC optimization," *IEEE Trans. Ind. Informat.*, vol. 15, no. 9, pp. 5289–5298, Sep. 2019.

[14] X. Xu, H. Jia, D. Wang, C. Y. David, and H.-D. Chiang, "Hierarchical energy management system for multi-source multi-product microgrids," *Renew. Energy*, vol. 78, pp. 621–630, Jun. 2015.

[15] Y. Wang, S. Mao, and R. M. Nelms, "On hierarchical power scheduling for the macrogrid and cooperative microgrids," *IEEE Trans. Ind. Informat.*, vol. 11, no. 6, pp. 1574–1584, Dec. 2015.

[16] Y. Xia, W. Wei, M. Yu, Y. Peng, and J. Tang, "Decentralized multi-time scale power control for a hybrid AC/DC microgrid with multiple subgrids," *IEEE Trans. Power Electron.*, vol. 33, no. 5, pp. 4061–4072, May 2018.

[17] P. Tian, X. Xiao, K. Wang, and R. Ding, "A hierarchical energy management system based on hierarchical optimization for microgrid community economic operation," *IEEE Trans. Smart Grid*, vol. 7, no. 5, pp. 2230–2241, Sep. 2016.

[18] Z. Yu, L. Jia, M. C. Murphy-Hoye, A. Pratt, and L. Tong, "Modeling and stochastic control for home energy management," *IEEE Trans. Smart Grid*, vol. 4, no. 4, pp. 2244–2255, Dec. 2013.

[19] F. Kennel, D. Görges, and S. Liu, "Energy management for smart grids with electric vehicles based on hierarchical MPC," *IEEE Trans. Ind. Informat.*, vol. 9, no. 3, pp. 1528–1537, Aug. 2013.

[20] V.-H. Bui, A. Hussain, and H.-M. Kim, "A multiagent-based hierarchical energy management strategy for multi-microgrids considering adjustable power and demand response," *IEEE Trans. Smart Grid*, vol. 9, no. 2, pp. 1323–1333, Mar. 2018.

[21] H. Wang and J. Huang, "Cooperative planning of renewable generations for interconnected microgrids," *IEEE Trans. Smart Grid*, vol. 7, no. 5, pp. 2486–2496, Sep. 2016.

[22] C. Zhang, Y. Xu, Z. Y. Dong, and K. P. Wong, "Robust coordination of distributed generation and price-based demand response in microgrids," *IEEE Trans. Smart Grid*, vol. 9, no. 5, pp. 4236–4247, Sep. 2018.

[23] S. Yousefi, M. P. Moghaddam, and V. J. Majd, "Optimal real time pricing in an agent-based retail market using a comprehensive demand response model," *Energy*, vol. 36, no. 9, pp. 5716–5727, 2011.

[24] J. Aghaei and M.-I. Alizadeh, "Multi-objective self-scheduling of chp (combined heat and power)-based microgrids considering demand response programs and esss (energy storage systems)," *Energy*, vol. 55, pp. 1044–1054, Jun. 2013.

[25] H. A. Aalami, M. P. Moghaddam, and G. R. Yousefi, "Demand response modeling considering interruptible/curtailable loads and capacity market programs," *Appl. Energy*, vol. 87, no. 1, pp. 243–250, 2010.

[26] E. Reihani, M. Motalleb, M. Thornton, and R. Ghorbani, "A novel approach using flexible scheduling and aggregation to optimize demand response in the developing interactive grid market architecture," *Appl. Energy*, vol. 183, pp. 445–455, Dec. 2016.

[27] C. Ju, P. Wang, L. Goel, and Y. Xu, "A two-layer energy management system for microgrids with hybrid energy storage considering degradation costs," *IEEE Trans. Smart Grid*, vol. 9, no. 6, pp. 6047–6057, Nov. 2018.

[28] K. Smith, M. Earleywine, E. Wood, J. S. Neubauer, and A. Pesaran, "Comparison of plug-in hybrid electric vehicle battery life across geographies and drive-cycles," vol. 1, SAE, Warrendale, PA, USA, Rep. NREL/CP-5400-53817, 2012, doi: 10.4271/2012-01-0666.

[29] M. Koller, T. Borsche, A. Ulbig, and G. Andersson, "Defining a degradation cost function for optimal control of a battery energy storage system," in *Proc. Grenoble PowerTech (POWERTECH)*, Grenoble, France, 2013, pp. 1–6.

[30] K. Heussen, S. Koch, A. Ulbig, and G. Andersson, "Unified system-level modeling of intermittent renewable energy sources and energy storage for power system operation," *IEEE Syst. J.*, vol. 6, no. 1, pp. 140–151, Mar. 2012.

[31] A. N. Venkat, I. A. Hiskens, J. B. Rawlings, and S. J. Wright, "Distributed MPC strategies with application to power system automatic generation control," *IEEE Trans. Control Syst. Technol.*, vol. 16, no. 6, pp. 1192–1206, Nov. 2008.

Yigao Du is currently pursuing the Ph.D. degree in control science and engineering with the Department of Automation, Shanghai Jiao Tong University, Shanghai, China. From 2018 to 2019, he was sponsored by China Scholarship Council to be a joint Ph.D. student with the Department of Energy Resources Engineering, Stanford University, Stanford, CA, USA. His research interests include control and optimization of cyber physical systems, with a recent focus on the analytics of renewable energy, operations and economics of microgrids, demand response, and energy management systems.

Jing Wu (Member, IEEE) received the B.S. degree in electrical engineering from Nanchang University in 2000, the M.S. degree in electrical engineering from Yanshan University in 2002, and the Ph.D. degree in electrical engineering from the University of Alberta in 2008. Since 2011, she has been with Shanghai Jiao Tong University, Shanghai, China, where she is currently an Associate Professor. She is a registered Professional Engineer in Alberta, Canada. Her current research interests include robust model predictive control, security control, and stability analysis and estimations for cyber-physical systems.

Shaoyuan Li (Senior Member, IEEE) received the B.S. and M.S. degrees in automation from the Hebei University of Technology, Tianjin, China, in 1987 and 1992, respectively, and the Ph.D. degree from the Department of Computer and System Science, Nankai University, Tianjin, in 1997. Since July 1997, he has been with the Department of Automation, Shanghai Jiao Tong University, Shanghai, China, where he is currently a Professor. His research interests include model predictive control, dynamic system optimization for large-scale networked systems. He is a Vice President of Asian Control Association.

Chengnian Long (Member, IEEE) received the B.S., M.S., and Ph.D. degrees in control theory and engineering from Yanshan University, China, in 1999, 2001, and 2004, respectively. He was a Research Associate with the Department of Computer Science and Engineering, Hong Kong University of Science and Technology and a Killam Postdoctoral Fellow with the University of Alberta, Canada. In 2009, he was with Shanghai Jiao Tong University, where he has been a Full Professor since 2011. His current research interests include cyber physical systems security, Internet of Things, and distributed intelligent systems.

Simona Onori (Senior Member, IEEE) received the Laurea degree (*summa cum laude*) in computer science engineering from the University of Rome 'Tor Vergata' in 2003, the M.S. degree in electrical and computer engineering from the University of New Mexico, Albuquerque, NM, USA, in 2004, and the Ph.D. degree in control engineering University of Rome 'Tor Vergata' in 2007. She has been an Assistant Professor with the Energy Resources Engineering Department, Stanford University since October 2017. She is a recipient of the 2019 Board of Trustees Award for Excellence, Clemson University, the 2018 Global Innovation Contest Award, LG Chem, the 2018 SAE Ralph R. Teetor Educational Award, the 2017 NSF CAREER Award, the 2017 Clemson University College of Engineering and Science Dean's Faculty Fellows Award, the 2017 Clemson University Esin Gulari Leadership & Service Award, the 2016 Energy Leadership Award in the category Emerging Leader (for the Carolinas), the 2015 Innovision Award (South Carolina), and the 2012 Lumley Interdisciplinary Research, 2011 Outstanding Technology Team Award, TechColumbus.